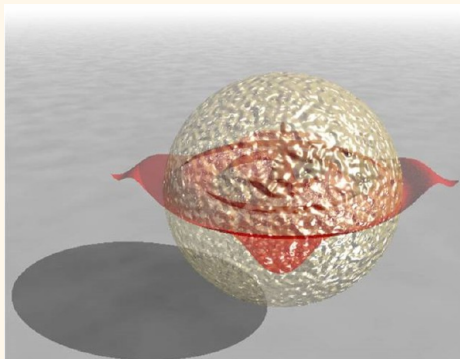


Localized Surface Plasmon Resonances in Spatially Dispersive Nano-Objects: Phenomenological Treatise

Pavel Ginzburg* and Anatoly V. Zayats

Department of Physics, King's College London, Strand, London WC2R 2LS, United Kingdom

ABSTRACT Nonlocal optical response of materials, important at the nanometric scale, influences numerous optical phenomena, such as electromagnetic field confinement and spectral characteristics of plasmonic resonances. Here, we present a general phenomenological approach to account for nonlocal material polarizabilities in nanoscale metal particles. The problem of nonlocal plasmonic resonances is formulated by an integro-differential equation in a space domain and solved by adopting its weak form, implemented in the finite element method, thus, dispensing with the requirements on additional boundary conditions. As an example, nonlocal smearing effects in plasmonic nanorods of various cross sections and nanotubes have been considered. Clear signature of nonlocality manifests itself in the interference fringes in the potential profile and a significant frequency shift of the localized surface plasmon resonances. These effects are especially important for nanoparticles with geometrical features comparable to the de Broglie wavelengths of electrons participating in the light–matter interactions. The proposed method provides a universal tool for phenomenological account of nonlocalities of any kind with the only requirement of linearity in system's response.



KEYWORDS: surface plasmon resonance · plasmonic nanoparticles · nonlocality · spatial dispersion

In electrodynamics, a susceptibility tensor describes material's response to applied electromagnetic fields. This tensor contains all the information required for description of electromagnetic properties of the material. Generally, it can be obtained either empirically or with classical or quantum models and depends on all time-space coordinates.¹ Moreover, the evaluation of this material response at a particular point in time and space requires the knowledge of all the history of the system (determined by chromatic dispersion) and the fields in the surroundings (determined by spatial dispersion). In optics, spatial dispersion is much weaker than chromatic one since characteristic dimensions of an electronic system interacting with light, *e.g.*, an atom or a molecule, are much smaller than an optical wavelength, while their energies may be comparable.² Typical material systems provide sufficient time delay and/or frequency filtering to an incident field that can be described by the wavelength-dependent real and imaginary parts of the refractive index, respectively. At the same time, these systems

may be almost insensitive to spatial orientation of the microscopic constituents with respect to any illumination angle, if polarization selection rules are ignored. Nevertheless, spatial dispersion can be important when light interacts with bulk material objects and gives rise to new phenomena, such as, *e.g.*, gyrotropy.²

Recently, various nanostructured media such as surfaces, films, and metamaterials,³ have been used to control light–matter interaction and to achieve advanced nanophotonic functionalities⁴ and transformation-optics designs.⁵ In many cases, nanostructured media are inherently spatially dispersive—this effect may originate either from the nonlocal dispersion of material components at the nanoscale² or from collective response of strongly coupled objects.^{6,7} The material contribution can in turn be approximately subdivided in classical nonlocality due to collective electronic effects and quantum one due to finite size of the electron wave function.

Classically, nonlocalities in optical response of a material originate from collective behavior of electron plasma, whose evolution can

* Address correspondence to pavel.ginzburg@kcl.ac.uk.

Received for review February 19, 2013 and accepted April 9, 2013.

Published online April 09, 2013
10.1021/nn400842m

© 2013 American Chemical Society

be well understood in the framework of the hydrodynamic model, considering the electron system as a charged fluid with certain average density and velocity.⁸ The pressure terms in this model are proportional to the gradient of the electron density and, hence, give rise to nonlocalities. The resulting modified Ohm's law contains nonlocal contributions, proportional to the Fermi velocity and can be used together with the Maxwell's equations to describe electromagnetic response. Other contributions to nonlocal response come from finite sizes of (quantum) wave functions describing objects interacting with light. Quantum nature of electronic system starts to manifest itself when characteristic dimensions of confining potentials are comparable with the coherence length of the electron wavepacket (Figure 1a), which is roughly equal to the electron de Broglie wavelength (or the Fermi wavelength in metals). As an example, one can consider excitons in semiconductors² or electron density tail outside the metal object boundary.⁹ Thus, nonlocalities in optical response of nanostructures could be of 'many-body/hydrodynamic', 'quantum', or 'structural' origin or of any combinations of the three.

Substantial theoretical and experimental progress has recently been made in the investigations of nonlocal contributions to optical response of metal nanostructures. For example, 'structural' nonlocality in arrays of strongly coupled wires or layers gives rise to strong spatial dispersion,^{6,7,10,11} which cannot be described by conventional effective medium models. Careful inclusion of spatial dispersion effects is demanded for description of various macroscopic effects, such as hyperlensing¹² or low frequency plasmonics.¹³ Furthermore, the predicted 'infinite' density of photonic states in hyperbolic metamaterials¹⁴ may, in fact, be limited not only by finite dimensionality of a unit cell,¹⁵ but also due to hydrodynamic-type of nonlocality.¹⁶

'Hydrodynamic' nonlocality can be straightforwardly included within classical electromagnetic modeling, as it directly depends on natural Maxwell's variables, specifically, electric field and current. However, the inclusion of the nonlocal Ohm's law imposes the requirement of the additional boundary conditions (the so-called 'ABC')¹ which corresponds to zero current outflow perpendicular to a boundary in the case of a metal. The ABC depend on a particular system under consideration.¹⁷ Taking into account these effects, the first numerical solutions for nonlocal nanoparticle resonances have been reported in McMahon *et al.*¹⁸ and shown remarkable differences in scattering cross sections of particles of different shapes. Similar approach has revealed the appearance of new types of plasmonic resonances with strong signature of additional oscillations in their extinction.¹⁹ The comprehensive numerical treatment of nonlocal effects in nanoparticles within hydrodynamic model has also been recently developed.²⁰ The phenomenon of the hydrodynamic

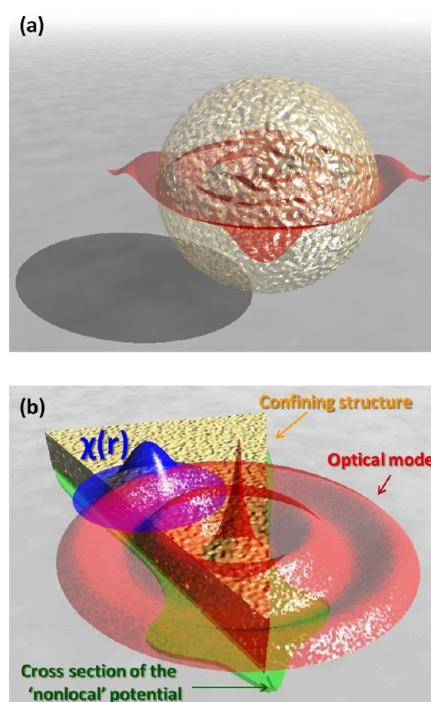


Figure 1. Schematic illustrating 'quantum' nonlocality: carrier wave function size is comparable with confining potential size. (b) Schematic illustrating the notion of nonlocal modal volume: (red) confined optical mode, (golden pattern) metallic wedge with (blue) nonlocal electron response leading to the redefined volume of the confining structure (green).

nonlocality can also affect nanoplasmonic waveguiding and focusing^{21–23} by effectively smearing sharp geometrical features of metallic nanostructures.²⁴

'Quantum' nonlocality in metals originates from the electron Fermi wavelength, which is of the order of few tenths of nanometer for noble metals.²⁵ In this case, particular attention has been paid to systems of coupled metal particles, as they may lead to unrealistic local field enhancement if been treated within the framework of local electromagnetic theory. However, careful account for quantum tunnelling on subnanometric scales (can be considered as nonlocality in this context) well describes experimental observations of the enhancement reduction.²⁶ The effects of non-Markovian dynamics of plasmonic resonances may also emerge as the result of quantum behavior.²⁷

The comprehensive theory of nonlocal contributions to electromagnetic response of nanostructures is still absent. Recent experimental observations show a need for a nonlocal description of nanoparticle's optical properties since they cannot be explained by conventional local theory. While much has already been done in this respect, the universal tool to treat a nonlocal susceptibility tensor of arbitrary type does not exist. Nevertheless, the most general response of a linear system (either classical or quantum) can be described as an integral of an excitation with a certain kernel (if vacuum fluctuations are ignored). Unfortunately, analytical solutions for electromagnetic scattering can only be found in

the simplest geometrical configurations, such as spheroid or cylinder, for only some particular types of nonlocality.^{28,29} Hence, advanced numerical approaches are required, especially, if optical properties of metals or semiconductors are studied.

In this paper, we propose a universal phenomenological approach for treatment of localized surface plasmons (LSPs) in spatially dispersive medium, employing the weak form solution of characteristic integro-differential counterpart of the Laplace equation. We restrict the discussion to the nonlocalities emerging from material properties of individual nanoscale objects, such as small metal particles. While previous approaches were limited to treatment of scattering phenomena, considering nonlocality in the Fourier domain with bounded spectrum of plane waves, we developed full eigenmode analysis, considering nonlocalities described in the space-domain. Moreover, we succeeded to avoid the need for the additional boundary conditions by formulating the problem in the whole space domain (not as a piecewise set of differential equations) and demanding certain continuity relations on separating boundaries. The example of smearing nonlocality in various metal nanoparticles has been considered in order to demonstrate the proposed approach.

RESULTS

Theoretical Framework. The general expression for the material polarizability $\vec{P}(\vec{r})$ taking into account all possible nonlocal effects is given by

$$\vec{P}(\vec{r}) = \varepsilon_0 \int \vec{\chi}_r(\vec{r}, \vec{r}') \vec{E}(\vec{r}') d^3r' \quad (1)$$

where $\vec{\chi}_r(\vec{r}, \vec{r}')$ is the nonlocal susceptibility tensor, ε_0 is the vacuum permittivity, and $\vec{E}(\vec{r}')$ is the electric field. For the sake of simplicity, the time dependence in our considerations is ignored as we deal with monochromatic fields in a linear regime. For bulk medium with translational symmetry, the kernel integral of eq 1 reduces to the convolution, where the scenario of $\vec{\chi}_r(\vec{r}, \vec{r}') \sim \delta(\vec{r} - \vec{r}')$ corresponds to a conventional local material response.

To illustrate how nonlocality influences the confined optical modes, we restrict the consideration to the quasistatic regime when the retardation effects can be ignored. Under this condition and including nonlocal effects, the electromagnetic mode can be described by the modified Laplace equation for the electric potential φ :

$$\nabla^2 \varphi + \nabla \cdot \left(\int \vec{\chi}_r(\vec{r}, \vec{r}') \vec{\nabla} \varphi(\vec{r}') d^3r' \right) = 0 \quad (2)$$

Assuming a metallic particle embedded in a local dielectric material (ε_d), we rewrite eq 2 as

$$\nabla^2 \varphi + \nabla \cdot (\theta(\vec{r}) \int_{\vec{r}, \vec{r}' \in M} \vec{\chi}_m(\vec{r}, \vec{r}') \vec{\nabla} \varphi(\vec{r}') d^3r') + \nabla \cdot ((1 - \theta(\vec{r}))(\varepsilon_d - 1) \vec{\nabla} \varphi(\vec{r})) = 0 \quad (3)$$

which reduces to the well-known expression in the case of local materials:³⁰

$$\nabla \cdot (\theta \vec{\nabla} \varphi) - \frac{\varepsilon_d}{(\varepsilon_d - \varepsilon_m)} \nabla^2 \varphi = 0 \quad (4)$$

where ε_m is the local dielectric constant of a metal. The last term in eq 3 results from the material polarizability of the surrounding medium and is responsible for creation of the local polarization charge at the boundary of a nanoparticle. This additional local contribution competes with nonlocal response and may smear its signature. In the case when an embedding medium is vacuum, the last summand of eq 3 is zero.

It is possible to reformulate integro-differential eq 3 in the so-called weak form³¹ by multiplying it by an arbitrary 'well-behaved' test function $\Phi(\vec{r})$, vanishing at infinity, and integrating over entire space. The resulting expression is

$$\int_V [\nabla \varphi(\vec{r}) \nabla \Phi(\vec{r}) + \theta(\vec{r}) \nabla \Phi(\vec{r}) \int_{\vec{r}, \vec{r}' \in M} \vec{\chi}_m(\vec{r}, \vec{r}') \vec{\nabla} \varphi(\vec{r}') d^3r'] + ((1 - \theta(\vec{r}))(\varepsilon_d - 1) \vec{\nabla} \varphi(\vec{r}) \nabla \Phi(\vec{r})) d^3r = 0 \quad (5)$$

Any kernel $\vec{\chi}_m(\vec{r}, \vec{r}')$ corresponding to a given physical effect (either 'many body/hydrodynamic', 'quantum' or 'structural') can be considered using eq 5. It can be numerically solved using, *e.g.*, finite element method to find the potential. In particular, in the examples below, the piecewise linear 'tent' (triangular) functions have been used as the basis with the triangular nonuniform mesh.³²

Equation 3 and its 'weak' form eq 5 describe a most general response of a linear system and can be analyzed within our approach without any additional assumptions. Phenomenological susceptibility tensor includes all possible physical effects. In the particular example described below, the geometrical aspects (smearing) were considered; all other effects will show off if appropriate susceptibility tensor is assumed. The proposed method is a universal tool that could be used for fitting any experimental data if sufficient amount of 'phenomenology' is provided. It can be used in the same way as one uses a standard phenomenological susceptibility for describing a conventional electromagnetic response, without a need to consider microscopic nature of susceptibility.

The Example of Smearing Nonlocality. As a proof of concept, we have considered the effects of a smearing nonlocality on LSP resonances. This type of nonlocality is appropriate for description of delocalized electron wave function and mostly influences nanostructures with sharp geometrical features, thin layers or small interparticle gaps.

First, we formulate a 'rule of thumb' to understand when the smearing nonlocality affects optical response of a nanostructure. For simplicity, we assume a two-material-body problem: one (generally, optically denser

and spatially dispersive) material, which confines an optical mode, is surrounded by different 'local' material. We define a geometrical shape function $\theta(\vec{r})$ equal to 1 inside the confining material volume Ω (e.g., a particle, a cavity or a waveguide) and 0 otherwise. The modal volume inside the spatially dispersive material can be then defined as

$$V_{in}(\theta(\vec{r})) = \frac{\int \theta(\vec{r}) |E(\vec{r})|^2 d^3r}{\max_{\Omega} \{|E(\vec{r})|^2\}} \quad (6)$$

This expression is different from the conventional mode volume definition of $V_{in}(\theta(\vec{r})) = \int_V \varepsilon(\vec{r}) |E(\vec{r})|^2 d^3r / \max_V \{\varepsilon(\vec{r}) |E(\vec{r})|^2\}$,³³ since it is designed to account for nonlocal effects taking place inside the confining medium. Now, again assuming material with translational symmetry, we define the 'smeared' shape function $\tilde{\theta}(\vec{r}) = \int \theta(\vec{r}') \tilde{\chi}_r(\vec{r} - \vec{r}') d^3r' / \int \tilde{\chi}_r(\vec{r}') d^3r'$, which is the normalized convolution of the geometrical shape function (initial confining potential) with the space profile of the spatially dispersive susceptibility tensor. In the case of $\tilde{\chi}_r(\vec{r}, \vec{r}') \sim \delta(\vec{r} - \vec{r}')$, there is no smearing due to nonlocal effects and $\theta = \tilde{\theta}$, as expected. We can then estimate the importance of nonlocality for a particular material configuration introducing the factor

$$\eta = \frac{V_{in}(\tilde{\theta}) - V_{in}(\theta)}{V_{in}(\theta)} \quad (7)$$

Whenever $\eta \sim 0$, the nonlocal contributions are negligible; otherwise, they should be taken into account. The simple physical meaning of the nonlocality contribution η is the relative spreading out of the confining potential from the limit of its geometrical boundaries, weighted with the field intensity of the mode (Figure 1b).

In the following, the nonlocal tensor has been taken in a general Gaussian scalar form

$$\chi_m(\vec{r}, \vec{r}') = (\bar{\varepsilon}_m - 1) \frac{1}{2\pi\xi^2} e^{-|\vec{r} - \vec{r}'|^2/2\xi^2} \quad (8)$$

where ξ is the effective radius of nonlocality, mimicking the measure of distance at which the fields in two points are correlated *via* the material response (e.g., delocalized electron wave function). The dielectric function $\varepsilon_m(\omega)$ generally differs from the local dielectric function ε_m of a bulk material and may depend on all parameters of the system. It can be obtained from microscopic or *ab initio* calculations taking into account hydrodynamic and/or quantum effects in nanoparticles of finite size.

For example, the theoretical model, used in the description of the recent experiments on size-dependent LSP spectral shift, adopts the approach of 'quantum particles in a box'. The confining potential has infinite barriers, coinciding with the boundaries of the particle. As the result of this semianalytical

approach, the effective 'local' permittivity of the particle is derived and subsequently substituted into the classical Mie theory, which predicts the blue shift of the LSP resonances with the decrease of particle's radius, supporting electron energy-loss spectroscopy (EELS) measurements.³⁴ While this 'local' model of nonlocality with the local permittivity $\bar{\varepsilon}_m(\omega)$ renormalized by quantum effects describes well the experimental data, it makes several crucial assumptions which could be relaxed with our universal approach. In particular, many body effects in the metal's electron plasma limit the electron coherence to the Fermi wavelength, which is almost 1 order of magnitude smaller than dimensions of the confining potential (*i.e.*, the particle's boundaries). While the 'particle in a box' model assumes the infinite coherence length, the smearing form of eq 8 takes into account (phenomenologically) the many-body contribution. In addition, the usage of effective local permittivity ignores the coupling of nonlocal effects with external electromagnetic excitation (illumination), while the general form of eq 3 formulates the problem self-consistently. Similarly, density functional theories³⁵ enable one to evaluate dielectric properties of clusters (renormalized $\bar{\varepsilon}_m(\omega)$) but do not provide a self-consistent electromagnetic formulation.

It needs to be emphasized that the 'corrected' $\bar{\varepsilon}_m$ (eq 8) is a local parameter and does not explicitly depend on the coordinates. The example of the smearing effects emphasizes the direct impact of nonlocality in self-consistent electromagnetic formulation and is not universal physical model, while, the most general kernel in eq 3 (not limited to the convolution) can be used in the framework of the proposed formalism without the introduction of a renormalized permittivity. In the case of smearing nonlocality (eq 8), the potential profiles calculated with eq 5 do not depend on the value of the modified dielectric constant ($\bar{\varepsilon}_m$), as they are the eigenfunctions in this formulation. However, the spectrum of the eigenvalues $\{\bar{\varepsilon}_m\}$ determines specific frequencies of LSP resonances *via* material dispersion and the correction model for $\bar{\varepsilon}_m$.

Quasistatic LSP resonances, being treated in the framework of the local Laplace equation, are independent of the overall particle size. The radiative losses are negligible for small particles (less than 20 nm radius for silver spheres). Hence, it is convenient to define certain dimensionless measure of nonlocality in the quasistatic regime, ξ/R , where R is the critical size of the nano-object. It should be noted that, for simple shapes, this measure is strictly related to the more general one defined by eq 7: e.g., $\eta \sim [1 + (\xi/R)]^3 - 1 \sim 3(\xi/R)$ for a dipolar resonance of a nanosphere and $\eta \sim [1 + (\xi/R)]^2 - 1 \sim 2(\xi/R)$ for a nanocylinder. For fixed nonlocality, this measure will become larger for smaller sizes of the objects. From practical point of view, the nonlocality radius is dictated by material properties, while the particle size can be controlled by fabrication. The increase of the nonlocality

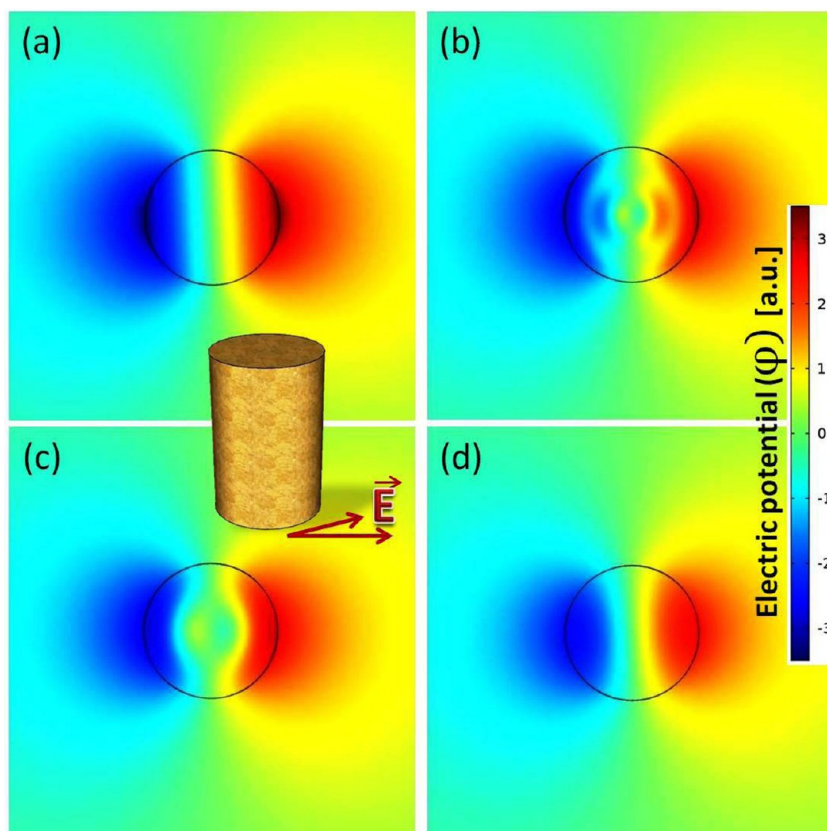


Figure 2. Potential φ map for the dipolar LSP resonance of a plasmonic nanocylinder with circular cross section (shown in the inset) for different nonlocality measures ξ/R : (a) local model ($\xi/R = 0$), (b) 0.1, (c) 0.2, and (d) 0.5. The color scale is the same for all images.

measure ξ/R corresponds to the increase of the nonlocality contribution to the optical properties, *i.e.*, the increase in η .

Equation 3, being formulated as the eigenvalue problem, enables estimation of the resonance shift with the introduction of a nonlocality. Since the LSP resonance has purely geometrical origin in quasistatic approximation, the resonant conditions are realized for certain values of $\bar{\epsilon}_m$, regardless of particular material components. Actual resonance frequency is determined by a particular material dispersion. For example, $\text{Re}(\bar{\epsilon}_m) = -2$ and $\text{Re}(\bar{\epsilon}_m) = -1$ are the dipolar LSP resonance conditions for sphere and cylinder, respectively, in vacuum, if local response is assumed with the renormalized by nonlocality $\bar{\epsilon}_m(\omega)$. Material and radiation losses, not entering the eigenvalue problem, will define quality factors of the resonances. Specific values of $\bar{\epsilon}_m$ could be further related to ϵ_m and resonant frequencies *via* specific correction models, as discussed above.

In the following, the smearing nonlocality was investigated in 3 different types of nanoparticles: nanocylinders with circular and concave cross sections and nanotubes.

Nonlocal Plasmonic Nanocylinder. The potential (φ) profiles calculated using eq 5 for dipolar LSP resonances in the cylinder of a circular cross section are

presented in Figure 2 for several nonlocality measures ξ/R , where R is the radius of the cylinder. In the local approximation (Figure 2a), the potential has a smooth profile as expected from the classical Laplace equation in piecewise continuous domain. The introduction of nonlocality (*cf.* eq 3 and eq 4) dramatically changes the potential profile which exhibits oscillatory behavior across the cylinder. Physically, these potential fringes correspond to the electron interference in the metal particle, while phenomenologically, as considered here, result from the 'memory' function (the integral operator in eq 3) which prevents the fast changes in the potential and, thus, causes oscillations. Remarkably, the number of fringes within the circular cross section is determined by the inverse nonlocality measure R/ξ . When the nonlocality measure reaches the critical point of 50%, the fringes disappear (Figure, 1d) as electrons are effectively shared within the whole particle.

Figure 4 shows the evolution of the LSP resonance condition as the nonlocality measure varies. It is remarkable that in the presence of smearing, the resonant values of $\bar{\epsilon}_m$ become more negative when nonlocality measure increases. This implies the red-shift contribution to the LSP spectral position with the decrease of the particle's radius and means that the smearing nonlocality is the competing mechanism

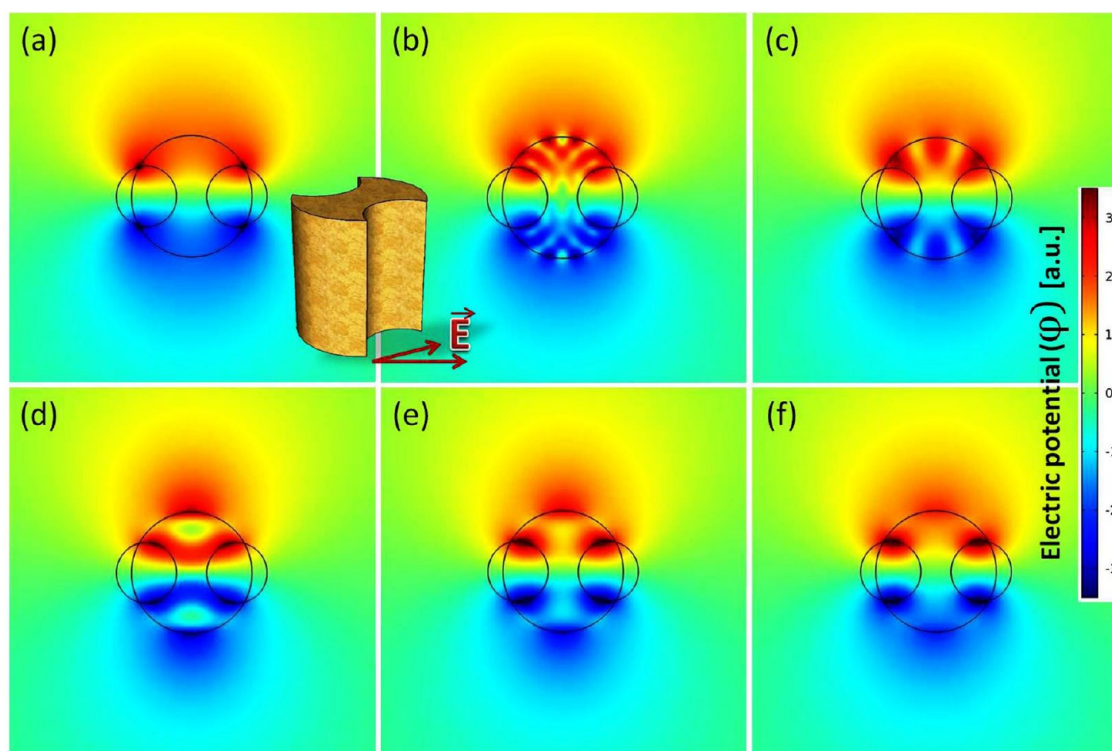


Figure 3. Potential ϕ map for the dipolar LSP resonance of a plasmonic nanocylinder with concave cross section (shown in the inset) for different nonlocality measures ξ/R : (a) local model ($\xi/R = 0$), (b) 0.1, (c) 0.2, (d) 0.4, (e) 0.5, and (f) 1. The concave cross section is formed by differentiation of circle of a normalized radius 2 with 2 circles of radius 1, symmetrically shifted by the distance of 1.5. The color scale is the same for all images.

to the other nonlocalities³⁴ which tend to blue-shift the resonance.

In the case of dark plasmonic modes, *e.g.*, quadrupolar LSP, it could be intuitively understood that the smearing nonlocality may have even more significant influence on the resonance shifts. They exhibit faster variation of a spatial profile of the potential inside the metal nanoparticles in contrast to the dipolar mode of nanospheres and nanocylinders which has uniform field and linear potential inside metal.

Nonlocal Plasmonic Nanoparticle with Sharp Corners. In contrast to particles with smooth convex cross sections, concave particles, which may provide any on demand spectrum,³⁶ could exhibit more complex nonlocal behavior as they possess sharp corners where critical dimensions become very small and comparable to the nonlocality radius even if the overall size of the particle may be larger. We can coin this scenario by the term “locally induced nonlocal effects”, when the optical response of large particle can be dictated by small sharp features of its geometry where the electromagnetic mode is localized. We will consider a cylinder with the concave cross section (Figure 3) formed by differentiation of a circle of radius 2 with 2 circles of radius 1, symmetrically shifted by the distance of 1.5 (all the radii are normalized). The effect of different measures of nonlocalities was modeled, and the interference patterns in the potential for the fundamental dipolar

resonance were observed. In this more complex scenario, the interference fringes exist even for large nonlocality measures, in contrast to the smooth convex circular cross section particles, and are the manifestation of existence of multiple boundaries of the particle. Electric field, being determined by the gradient of the potential, is very sensitive to the oscillations of the potential. The consideration of the potential variations near the sharp corners allows predicting reduction of the local fields. The LSP resonance shift due to the smearing nonlocality is shown in Figure 4. The actual LSP resonances of concave particles are also red-shifted with respect to the convex ones, as was demonstrated both theoretically and experimentally.³⁷

Nonlocal Plasmonic Nanotube. Plasmonic nanoshells and nanotubes with extremely thin metal layers of the order of few nanometers have recently been fabricated and are important for numerous applications. Nanoshell's optical properties are advantageous for gene silencing,³⁸ enhanced Raman spectroscopy,³⁹ nanomedicine,⁴⁰ low-energy water heating,⁴¹ achieving magnetic responses at optical frequencies,^{42,43} to name a few. Nanotubes are beneficial for efficient biosensing,⁴⁴ photovoltaics, and nonlinear nano-optics, and sensing applications.⁴⁵

For such layered nanostructures, the electron Fermi wavelength may become comparable with critical structural dimensions, thin shell layers or small cores,

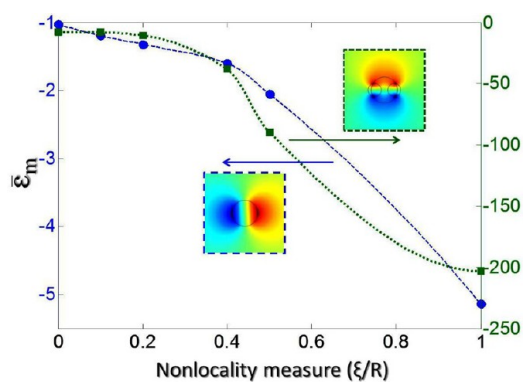


Figure 4. Parametric dependence of the resonant conditions for dipolar LSP resonance of a circular cross section cylinder (blue circles, dashed line) and a concave cross section cylinder (green rectangles, dotted line) on the nonlocality measure. Symbols are numerical simulations, and lines are guide for eye.

giving rise to strong nonlocal effects. In the following, we investigate 'bonding' and 'antibonding' resonances⁴⁶ of a metal nanotube corresponding to parallel and antiparallel dipoles induced at outer and inner boundaries, respectively, by varying either overall diameter of a nanotube, keeping the ratio between inner and outer radii constant, or fixing the outer radius and varying the thickness of the tube wall (Figure 5). Similar geometries were recently used for studies of hydrodynamic nonlocalities in applications to refractive index sensing.⁴⁷

First, we consider the tube with the ratio of outer and inner radii of 2:1.5 and vary the diameter. The dependence of the resonance position on the nonlocality measure is presented in Figure 5. The respective potential maps are shown in the insets. Remarkable negative shifts of ϵ_m'' occur for the LSP in nanotubes due to the nonlocal effects, as the electric field penetrates more into the metal shell. While for 'antibonding' mode the field drops substantially inside the tube, it becomes smaller on the outside for the 'bonding' resonance. Moreover, since the 'antibonding' mode supports much faster changes of the electric potential inside the tube walls (surface charge changes sign from outer to inner boundary in the local regime), the associated resonance shifts faster as the nonlocality smear out the field gradients. The results presented in Figure 5 predict the increase of the field inside the tube for the bonding resonance, while the opposite behavior takes place for the antibonding mode, for which the field is pushed away from the core with the increase of the nonlocality measure.

The nanotube has two key geometrical dimensions, giving rise for nonlocal contributions: wall thickness and core radius. Either thin walls or small core comparable with the Fermi wavelength will contribute to the nonlocal modification of the optical response. For the nanotube with the fixed outer radius of 20 nm, the inner radius has been varied in the range from 19 nm

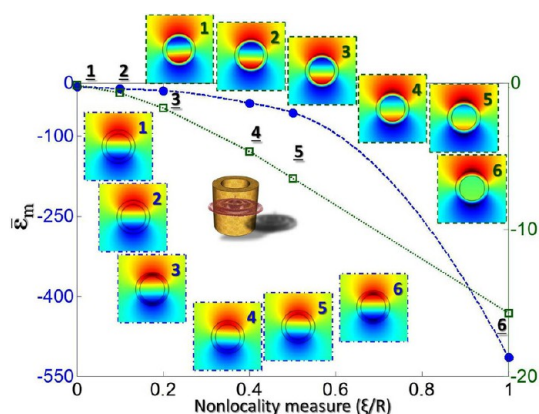


Figure 5. Parametric dependence of the resonant conditions for 'bonding' (blue circles, dashed line) and 'antibonding' (green rectangles, dotted line) LSP resonances of the nanotube on the nonlocality measure. Symbols are numerical simulations, and lines are guide for eye. The numbered insets show the potential ϕ profiles for different nonlocality measures.

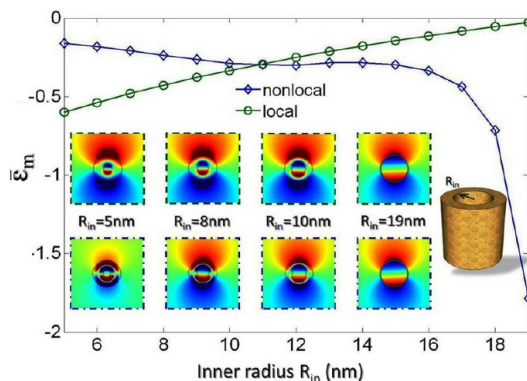


Figure 6. Parametric dependence of the resonant conditions for 'antibonding' LSP resonance of the nanotube on the inner radius (the outer radius is fixed to 20 nm): (blue diamonds, solid line) nonlocality with $\xi = 1$ nm, (green circles) without nonlocality. Symbols are numerical simulations, and lines are guide for eye. Potential ϕ profiles for several nanotube parameters are shown in the inset.

(very thin walls) to 6 nm (very small core). The nanotubes with similar dimensions can routinely be fabricated.⁴⁸ The parametric plots of the LSP resonant conditions (for ϵ_m'') for the 'antibonding' mode, which is more influenced by the nonlocal effects, are presented in Figure 6 for both local and nonlocal scenarios. We used $\xi = 1$ nm which is of the same order of magnitude as for noble metals. The resonant condition for this mode in the local regime, obtained with the use of Laplace equation, is $\epsilon_m = -[(R_{in} + R_{out})/(R_{out} - R_{in})]$ if embedded in vacuum. This dependence perfectly coincides with the numerical simulations implemented using eq 6. The results summarized in Figure 6 show that the local LSP position approaches the nonlocal one with the increase of the wall thickness from 1 to 10 nm, as the radius of nonlocality becomes less than the wall width. At the same time, with reduction of the inner radius, the tube core becomes smaller,

approaching size where the nonlocality starts to contribute again. This is the reason of the crossing point in the resonant conditions between local and nonlocal descriptions and subsequent significant dissimilarity with continuing decrease of the inner radius.

DISCUSSION

The universal approach formulated with eq 3 enables to account for nonlocality of any type. Smearing effects introduced by eq 8 are particular example of nonlocal response and their manifestation in optical properties strongly depends on considered physical system. In the case of convex particles with simple shapes (e.g., sphere, cylinder or disk), the smearing effects are less pronounced and compete with the permittivity changes due to other, e.g., finite size, effects. The overall result, according to the recent experimental observation,³⁴ will be a blue-shift of the LSP resonances with the decrease of the particle's dimensions.

The scenario of two closely situated tunnelling-coupled particles exhibits different behavior with the red shift of the LSP resonances. The smearing nonlocality is of particular significance for this scenario as the interaction is determined by the small gap between the particles. Hydrodynamic model was employed in order to describe the electron smearing in the tunnelling regime and predicted the red shift of the LSP resonances with the decrease of the tunnelling gap (i.e., the increase of the nonlocality measure ξ/R).^{49,50} Hydrodynamic model enables to produce qualitative predictions using compact and universal (yet phenomenological) formulation. It introduces the nonlocality in the form of the set of coupled differential equations and enables to keep both the material and electromagnetic properties together. It was recently shown by Mortensen *et al.* that this set of equations can be recast either with the Green's functions⁵¹ or operator⁵² approaches.

It should be noted, however, that several assumptions on quantum pressure term were made in Eguiluz and Quinn⁸ in order to represent the hydrodynamic model in compact and numerically solvable form. The hydrodynamic equations rely only on the gradient term which introduces nonlocality *via* the information on the closest neighbor. This implies that the nonlocal approach developed by Eguiluz and Quinn⁸ cannot be directly related to the model we presented above, as our model depends on the collective response from the certain surrounding and not just on the closest points in the virtual grid. The direct comparison between hydrodynamic model and our approach is not straightforward as it would involve the knowledge on the overall field in a particular system that needs to be solved first.

CONCLUSION

We have developed a new approach that enables investigations of localized surface plasmon resonances of linear systems with a general nonlocal susceptibility

tensor. An integro-differential equation describing nonlocal electromagnetic properties has been solved numerically by adopting its weak form.

Considering the example of smearing nonlocality, we have formulated the criterion to estimate whenever this phenomenon influences optical responses of nanostructures. Clear signature of the smearing nonlocality has been observed as the interference fringes in the potential profile of the localized plasmonic excitations. The investigations of nanocylinders and nanotubes with various cross sections leads to the conclusion that smearing has significant influence on LSP position, shifting the resonances, as characteristic features of the objects approach nonlocality radius determined by the de Broglie wavelength of carriers interacting with electromagnetic field. It is also shown that other types of nonlocalities, which may result in renormalization of the nano-object's permittivity with respect to bulk material permittivity, need to be simultaneously considered to explain the experimental observations.

Conflict of Interest: The authors declare no competing financial interest.

Acknowledgment. This work has been supported, in part, by EPSRC (U.K.). P. Ginzburg acknowledges support from The Royal Society *via* the Newton International Fellowship.

REFERENCES AND NOTES

- Landau, L. D.; Lifshitz, E. M. *Electrodynamics of Continuous Media*; Pergamon Press: New York, 1960.
- Agranovich, V. M.; Ginzburg, V. L. *Spatial Dispersion in Crystal Optics and the Theory of Excitons*; Springer-Verlag: Berlin, 1984.
- Sarychev, A. K.; Shalaev, V. M. *Electrodynamics of Metamaterials*; World Scientific: Singapore, 2007.
- Curto, A. G.; Volpe, G.; Taminiau, T. H.; Kreuzer, M. P.; Quidant, R.; van Hulst, N. F. Unidirectional Emission of a Quantum Dot Coupled to a Nanoantenna. *Science* **2010**, *329*, 930–933.
- Pendry, J. B.; Schurig, D.; Smith, D. R. Controlling Electromagnetic Fields. *Science* **2006**, *312*, 1780–1782.
- Belov, P. A.; Marques, R.; Maslovski, S. I.; Nefedov, I. S.; Silverincha, M.; Simovski, C. R.; Tretyakov, S. A. Strong Spatial Dispersion in Wire Media in the Very Large Wavelength Limit. *Phys. Rev. B* **2003**, *67*, 113103.
- Pollard, R. J.; Murphy, A.; Hendren, W. R.; Evans, P. R.; Atkinson, R.; Wurtz, G. A.; Zayats, A. V.; Podolskiy, V. A. Optical Nonlocalities and Additional Waves in Epsilon-Near-Zero Metamaterials. *Phys. Rev. Lett.* **2009**, *102*, 127405.
- Eguiluz, A.; Quinn, J. J. Hydrodynamic Model for Surface Plasmons in Metals and Degenerate Semiconductors. *Phys. Rev. B* **1976**, *14*, 1347–1361.
- Marinica, D. C.; Kazansky, A. K.; Nordlander, P.; Aizpurua, J.; Borisov, A. G. Quantum Plasmonics: Nonlinear Effects in the Field Enhancement of a Plasmonic Nanoparticle Dimer. *Nano Lett.* **2012**, *12*, 1333–1339.
- Wurtz, G. A.; Pollard, R.; Hendren, W.; Wiederrecht, G. P.; Gosztola, D. J.; Podolskiy, V. A.; Zayats, A. V. Designed Ultrafast Optical Nonlinearity in a Plasmonic Nanorod Metamaterial Enhanced by Nonlocality. *Nat. Nanotechnol.* **2011**, *6*, 107–111.
- Elser, J.; Podolskiy, V. A.; Salakhutdinov, I.; Avrutsky, I. Nonlocal Effects in Effective-Medium Response of Nanolayered Metamaterials. *Appl. Phys. Lett.* **2007**, *90*, 191109.
- Jacob, Z.; Alekseyev, L. V.; Narimanov, E. E. Optical Hyperlenses: Far-Field Imaging beyond the Diffraction Limit. *Opt. Express* **2006**, *14*, 8247–8256.

13. Pendry, J. B.; Holden, A. J.; Stewart, W. J.; Youngs, I. Extremely Low Frequency Plasmons in Metallic Mesostuctures. *Phys. Rev. Lett.* **1996**, *76*, 4773–4776.
14. Jacob, Z.; Kim, J.; Naik, G. V.; Boltasseva, A.; Narimanov, E. E.; Shalae, V. M. Engineering Photonic Density of States Using Metamaterials. *Appl. Phys. B: Lasers Opt.* **2010**, *100*, 215.
15. Poddubny, A. N.; Belov, P. A.; Ginzburg, P.; Zayats, A. V.; Kivshar, Y. S. Microscopic Model of Purcell Enhancement in Hyperbolic Metamaterials. *Phys. Rev. B* **2012**, *86*, 035148.
16. Yan, W.; Wubs, M.; Mortensen, N. A. Hyperbolic Metamaterials: Nonlocal Response Regularizes Broadband Super-singularity. *Phys. Rev. B* **2012**, *86*, 205429.
17. Maslovski, S. I.; Morgado, T. A.; Silveirinha, M. G.; Kaipa, C. S. R.; Yakovlev, A. B. Generalized Additional Boundary Conditions for Wire Media. *New J. Phys.* **2010**, *12*, 113047.
18. McMahon, J. M.; Gray, S. K.; Schatz, G. C. Nonlocal Optical Response of Metal Nanostructures with Arbitrary Shape. *Phys. Rev. Lett.* **2009**, *103*, 097403.
19. Raza, S.; Toscano, G.; Jauho, A.; Wubs, M.; Mortensen, N. A. Unusual Resonances in Nanoplasmonic Structures due to Nonlocal Response. *Phys. Rev. B* **2011**, *84*, 121412(R).
20. Toscano, G.; Raza, S.; Jauho, A.; Mortensen, N. A.; Wubs, M. Modified Field Enhancement and Extinction by Plasmonic Nanowire Dimers due to Nonlocal Response. *Opt. Express* **2012**, *20*, 4176–4188.
21. Stockman, M. I. Nanofocusing of Optical Energy in Tapered Plasmonic Waveguides. *Phys. Rev. Lett.* **2004**, *93*, 137404.
22. Ginzburg, P.; Arbel, D.; Orenstein, M. Gap Plasmon Polariton Structure for very Efficient Microscale-to-Nanoscale Interfacing. *Opt. Lett.* **2006**, *31*, 3288–3290.
23. Ginzburg, P.; Orenstein, M. Plasmonic Transmission Lines: From Micro to Nano Scale with $1/4$ Impedance Matching. *Opt. Express* **2007**, *15*, 6762–6767.
24. Wiener, A.; Fernández-Domínguez, A. I.; Horsfield, A. P.; Pendry, J. B.; Maier, S. A. Nonlocal Effects in the Nanofocusing Performance of Plasmonic Tips. *Nano Lett.* **2012**, *12*, 3308–3314.
25. Mizutani, U. *Introduction to the Electron Theory of Metals*; Cambridge University Press: Cambridge, U.K., 2001.
26. Savage, K. J.; Hawkeye, M. M.; Esteban, R.; Borisov, A. G.; Aizpurua, J.; Baumberg, J. J. Revealing the Quantum Regime in Tunnelling Plasmonics. *Nature* **2012**, *491*, 574.
27. Ginzburg, P.; Zayats, A. V. Non-Exponential Decay of Dark Localized Surface Plasmons. *Opt. Express* **2012**, *20*, 6720–6727.
28. Ruppin, R. Optical Properties of a Spatially Dispersive Cylinder. *J. Opt. Soc. Am. B* **1989**, *6*, 1559–1563.
29. Boardman, A. D.; Paranjape, B. V. The Optical Surface Modes of Metal Spheres. *J. Phys. F* **1977**, *7*, 1935.
30. Bergman, D. J.; Stockman, M. I. Surface Plasmon Amplification by Stimulated Emission of Radiation: Quantum Generation of Coherent Surface Plasmons in Nanosystems. *Phys. Rev. Lett.* **2003**, *90*, 027402.
31. Silvester, P. P.; Ferrari, R. L. *Finite Elements for Electrical Engineers*. 3rd ed., Cambridge University Press, Cambridge, 1990.
32. <http://www.comsol.com/>.
33. Yariv, A.; Yeh, P. *Photonics: Optical Electronics in Modern Communications*; Oxford University Press: New York, 2007.
34. Scholl, J. A.; Koh, A. L.; Dionne, J. A. Quantum Plasmon Resonances of Individual Metallic Nanoparticles. *Nature* **2012**, *483*, 421–427.
35. He, Y.; Zeng, T. First-Principles Study and Model of Dielectric Functions of Silver Nanoparticles. *J. Phys. Chem. C* **2010**, *114*, 18023–18030.
36. Ginzburg, P.; Berkovitch, N.; Nevet, A.; Shor, I.; Orenstein, M. Resonances On-Demand for Plasmonic Nano-Particles. *Nano Lett.* **2011**, *11*, 2329–2333.
37. Berkovitch, N.; Ginzburg, P.; Orenstein, M. Concave Plasmonic Particles: Broad-Band Geometrical Tunability in the Near-Infrared. *Nano Lett.* **2010**, *10*, 1405–1408.
38. Huschka, R.; Barhoumi, A.; Liu, Q.; Roth, J. A.; Ji, L.; Halas, N. J. Gene Silencing by Gold Nanoshell-Mediated Delivery and Laser-Triggered Release of Antisense Oligonucleotide and siRNA. *ACS Nano* **2012**, *6*, 7681–7691.
39. Krohne-Nielsen, P.; Novikov, S. M.; Beermann, J.; Morgen, P.; Bozhevolnyi, S. I.; Albrechtsen, O. Surface-Enhanced Raman Microscopy of Hemispherical Shells Stripped from Templates of Anodized Aluminium. *J. Raman Spectrosc.* **2012**, *43*, 834–841.
40. Halas, N. J. The Photonic Nanomedicine Revolution: Let the Human Side of Nanotechnology Emerge. *Nanomedicine* **2009**, *4*, 369–371.
41. Neumann, O.; Urban, A. S.; Day, J.; Lal, S.; Nordlander, P.; Halas, N. J. Solar Vapor Generation Enabled by Nanoparticles. *ACS Nano* **2013**, *7*, 42–49.
42. Mirin, N. A.; Ali, T. A.; Nordlander, P.; Halas, N. J. Perforated Semishells: Far Field Directional Control and Optical Frequency Magnetic Response. *ACS Nano* **2010**, *4*, 2701.
43. Levin, C. S.; Hoffman, C.; Ali, T. A.; Kelly, A. T.; Morosan, E.; Nordlander, P.; Whitmire, K. H.; Halas, N. J. Magnetic-Plasmonic Core-Shell Nanoparticles. *ACS Nano* **2009**, *3*, 1379.
44. McPhillips, J.; Murphy, A.; Jonsson, M. P.; Hendren, W. R.; Atkinson, R.; Hook, F.; Zayats, A. V.; Pollard, R. J. High-Performance Biosensing Using Arrays of Plasmonic Nanotubes. *ACS Nano* **2010**, *4*, 2210–2216.
45. Murphy, A.; Sonnefraud, Y.; Krasavin, A. V.; Ginzburg, P.; Morgan, F.; McPhillips, J.; Wurtz, G.; Maier, S. A.; Zayats, A. V.; Pollard, R. J. Fabrication and Optical Properties of Large-Scale Arrays of Gold Nanocavities Based on Rod-in-a-Tube Coaxial. *Appl. Phys. Lett.* **2013**, *102*, 103103.
46. Prodan, E.; Radloff, C.; Halas, N. J.; Nordlander, P. A Hybridization Model for the Plasmon Response of Complex Nanostructures. *Science* **2003**, *302*, 419–422.
47. Raza, S.; Toscano, G.; Jauho, A.; Mortensen, N. A.; Wubs, M. Refractive-Index Sensing with Ultrathin Plasmonic Nanotubes. *Plasmonics* **2012**, *10*.1007/s11468-012-9375-z.
48. Murphy, A.; McPhillips, J.; Hendren, W.; McClatchey, C.; Atkinson, R.; Wurtz, G.; Zayats, A. V.; Pollard, R. J. The Controlled Fabrication and Geometry Tunable Optics of Gold Nanotube Arrays. *Nanotechnology* **2011**, *22*, 045705.
49. Ciraci, C.; Hill, R. T.; Mock, J. J.; Urzhumov, Y.; Fernández-Domínguez, A. I.; Maier, S. A.; Pendry, J. B.; Chilkoti, A.; Smith, D. R. Probing the Ultimate Limits of Plasmonic Enhancement. *Science* **2012**, *337*, 1072–1074.
50. Zuloaga, J.; Prodan, E.; Nordlander, P. Quantum Description of the Plasmon Resonances of a Nanoparticle Dimer. *Nano Lett.* **2009**, *9*, 887–891.
51. Mortensen, N. A.; Toscano, G.; Raza, S.; Stenger, N.; Yan, W.; Jauho, A.-P.; Xiao, S.; Wubs, M. Nanophotonics beyond Ohm's Law. *AIP Conf. Proc.* **2012**, *1475*, 28–32.
52. Toscano G.; Raza S.; Yan W.; Jeppesen C.; Xiao S.; Wubs M.; Jauho A.-P.; Bozhevolnyi S. I.; Mortensen N. A. Nonlocal Response in Plasmonic Waveguiding with Extreme Light Confinement. **2012**, arXiv:1212.4925.